Smart Elastic Fabric Strip Encompassing Pre-Strained Fiber Bragg Grating Sensors

Bastien Van Esbeen, Damien Kinet, Corentin Guyot, Annick Depré, Rik Knoppers, Remco Nieuwland, and Christophe Caucheteur

***Abstract*— This paper describes the creation and characterization of a smart elastic fabric strip that incorporates pre-strained fiber Bragg grating (FBG) sensors. The fabric strip is 700 mm long and 60 mm wide, and a standard single-mode optical fiber with four cascaded and wavelength-division-multiplexed gratings is sewn onto the strip. Each FBG sensor is affixed to a specifically-designed 3D-printed pad in a pre-strained manner, which permits the detection of both FBG traction and compression. Among three configurations, the design of the pad has been chosen following tensile tests. The sensitivity of the elastic fabric strip was measured, and it is found that there is a Bragg wavelength deviation of 12.2 pm per mm of textile elongation and 11.7 pm per mm in release. Validation tests are conducted to demonstrate the system sensitivity to compression: indeed, a negative Bragg wavelength shift compared to the rest position can be observed. Afterwards, ten traction cycles are applied to the fabric strip to validate its ability to repeat measurements in a dynamic setting. In stretched position, the standard deviation of the Bragg wavelength shifts from all the cycles is 2.46 pm. Similarly, in the rest position, the standard deviation is 0.60 pm. Finally, tests are performed in the context of backbone monitoring and results are analyzed for four backbone positions. These experiments pave the way to the use of the smart elastic band for the dynamic measurement of the backbone position of a patient.**

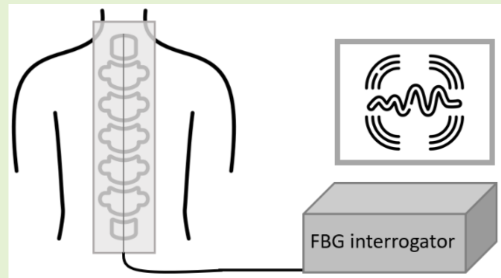

***Index Terms*— Backbone monitoring, fiber Bragg gratings, smart textile, strain sensing.**

I. Introduction

FIBER Fiber Bragg grating (FBG) sensors are becoming increasingly popular due to their many benefits, including their small size, robustness, immunity to electromagnetic interference, wavelength-encoded information, among others. These sensors are being used in a variety of practical applications, with strain, temperature, and bending sensing being the most common examples, but FBG technology is also well-suited for (bio)chemical sensing. Optical fibers, including FBGs, are ideal for use within or on top of textiles. As a result, there is growing interest in using fiber optic sensors embedded in textiles for a large set of applications, e.g. geotechnical engineering [1], structural health monitoring [2], [3], and mainly medical applications [4], [5], [6], [7], [8], [9], [10], such as respiratory monitoring [11], [12], [13], [14], [15]. Moreover, in [16], an FBG-based sensing system is proposed to monitor sitting positions and estimate the respiratory rate.

In this work, a novel smart fabric strip containing four pre-strained FBGs is presented. This allows to measure deformation levels highly larger than bare optical fibers can withstand (~3% elongation), at different positions along the fabric strip length. The case of backbone monitoring, among others, is therefore particularly suitable for our smart fabric strip. FBGs are naturally chosen compared to other optical strain sensing technologies such as Brillouin due to the more affordable interrogation techniques and the limited sensing length (less than one meter).

The paper provides an overview of FBG sensors and their working principles, as well as the integration of optical fibers into the textile and the fabrication design of the sensing system. The study then describes the calibration of the sensing setup in the lab, which is conducted to determine the sensitivity of the sensing system in terms of the Bragg wavelength shift [pm] per unit of elastic fabric elongation [mm]. Finally, validation tests are performed with the aim to confirm the compression sensing capabilities, the measurements repeatability of the sensing system and the good operation in the practical context of backbone monitoring.

II. FBG background

A fiber Bragg grating (FBG) is created by permanently

This paragraph of the first footnote will contain the date on which you submitted your paper for review. It will also contain support information, including sponsor and financial support acknowledgment. For example, "This work was supported in part by the U.S. Department of Commerce under Grant BS123456."

The next few paragraphs should contain the authors' current affiliations, including current address and e-mail. For example, F. A. Author is with the National Institute of Standards and Technology, Boulder, CO 80305 USA (e-mail: author@ boulder.nist.gov).

S. B. Author, Jr., was with Rice University, Houston, TX 77005 USA. He is now with the Department of Physics, Colorado State University, Fort Collins, CO 80523 USA (e-mail: author@lamar.colostate.edu).

T. C. Author is with the Electrical Engineering Department, University of Colorado, Boulder, CO 80309 USA, on leave from the National Research Institute for Metals, Tsukuba, Japan (e-mail: author@nrim.go.jp).

modifying the core refractive index inside an optical fiber in a periodic pattern. This modification acts as a distributed mirror, reflecting only a small portion of the incident light at a specific wavelength known as the Bragg wavelength (λ_B), while transmitting all other wavelengths. An FBG is defined by its grating period (Λ), grating length (L), and refractive index modulation (δ_n). The Bragg wavelength can be calculated by using

$$\lambda_B = 2(n_{eff} + \delta_n)\Lambda \approx 2n_{eff} \quad (1)$$

where n_{eff} is the effective refractive index of the core. When there is a variation in either n_{eff} or Λ, a Bragg wavelength shift is observed. This shift can be utilized for measuring axial strain, temperature, or pressure. The sensitivity of FBG to strain and temperature is linear, with typical values of respectively 1.2 pm/με and 10 pm/°C, at a wavelength of 1550 nm.

III. Textile strip fabrication and sensor integration

The company Elasta from Waregem, Belgium, manufactured the elastic fabric strip which measures 700 mm in length and 60 mm in width. It is made of polyester thread and natural gum. Four Bragg gratings are inscribed in a telecommunication-grade single-mode optical fiber. The amount of 4 is a good trade-off for easy data processing, while ensuring good spatial resolution and continuity of deformations between FBGs. Also, for future works, it enables the possibility of using an even cheaper and handier smart interrogator (portable, battery-operated, limited spectral range, etc) for which only a couple of sensors can fit in the spectral range. The use of conventional single-mode fiber suits interrogators based on standard components.

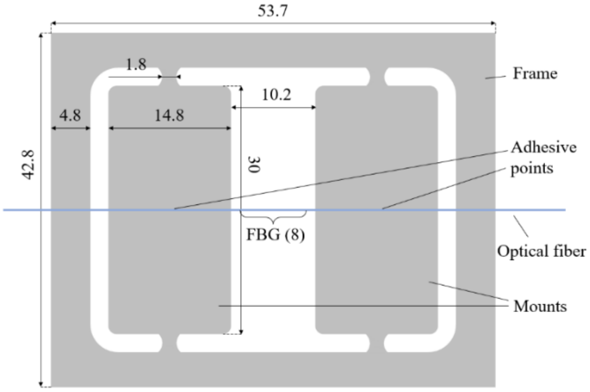

Fig. 1. Top view design of the 3D-printed pad with lengths in mm.

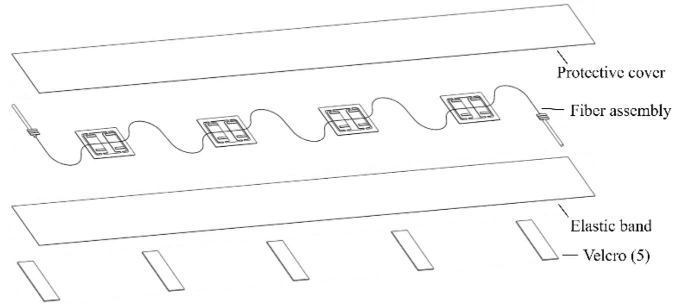

Fig. 2. Scheme of the elastic fabric strip in layers.

Each grating is attached to a specific 3D-printed pad of which the top view design is depicted in Fig. 1, where the distances are expressed in mm. The pad, made of PLA, is composed of two mounts (14.8 mm over 30 mm) attached to a frame (53.7 mm over 42.8 mm, and side width of 4.8 mm) by a 1.8 mm wide connection. The thickness of the structure is 0.75 mm. The fiber is horizontally (with respect to Fig. 1) bonded to the pad thanks to two adhesive points on the mounts with the FBG between them. The bonding was achieved by means of *Loctite* adhesive. The grating length is 8 mm, preventing any portion of the grating from being glued on a mount as the distance between them is 10.2 mm. This avoids any possible chirp of the grating. The pads are then sewn onto the fabric strip, in such a way that the gratings are separated from each other by a few centimeters of loss fiber, which becomes stretched when the fabric is in traction.

A scheme of the whole sensing system design in layers is provided in Fig. 2. Fig. 3 represents the reflected spectrum of the gratings integrated in the resulting design which can be

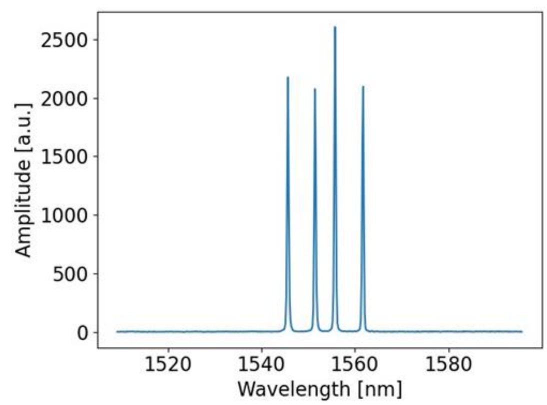

Fig. 3. Reflection spectrum of the four gratings integrated in the smart textile.

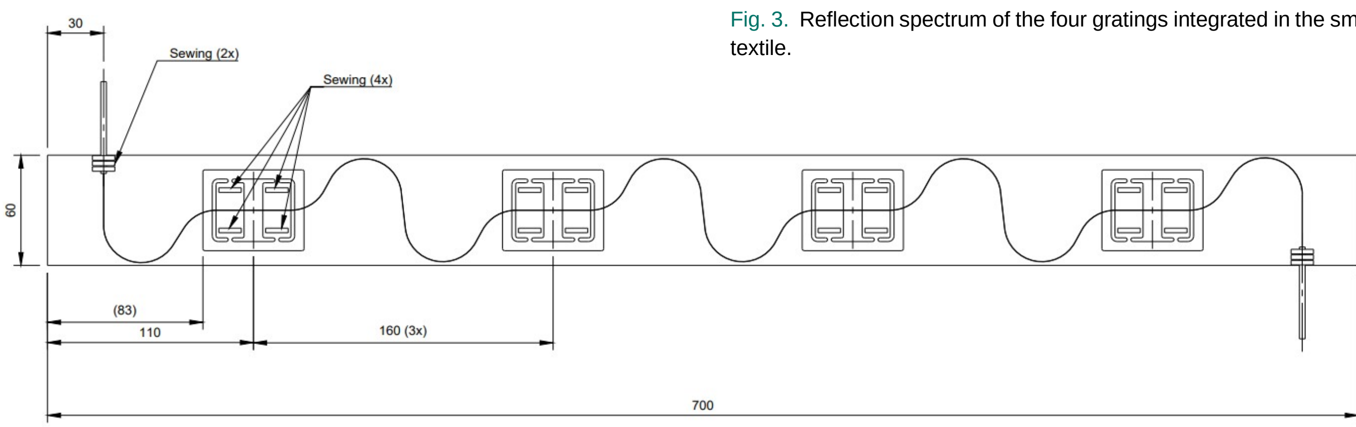

Fig. 4. Resulting scheme and sizes (in mm) of the fabric strip design.

found in Fig. 4, where the distances are expressed in mm. The spectrum before the integration is similar since only a pure axial pre-stress was applied, inducing a wavelength shift with no spectral distortion. Even if the design was primarily created for backbone monitoring, the concept of pre-strained textile sensors can be applied to various applications that require strain sensing on planar or curved surfaces.

In [16], a similar backbone monitoring solution based on an unobtrusive sensing device composed of a chain of seven FBGs was proposed for three sitting working positions and was very successfully tested. The sensors are placed on the skin and are also able to estimate the respiratory rate. For comparison, we are exploring the possibilities of spine monitoring in the standing position in addition to sitting. Also, our work enables the sensors to be installed on a cloth, preventing subjects from being potentially inconvenienced by the installation of devices on their skin.

Based on this design, a study of the FBG sensitivity implied by different pad schemes was performed. The pad acts as an anchor for the optical fiber on the textile while facilitating the pre-strain process of the FBG. Three configurations were designed, differing in the way the pad is sewn into the strip. The first configuration is characterized by two straight seams (100% polyester threads) while the other two show zigzag patterns. In configuration 2, the seams run only along the mounts while in configurations 1 and 3, they run along the mounts and the piece of fabric strip between them. Tensile tests were carried out for each configuration by applying two cycles with loads from 0 to 300 g by steps of 100 g and recording the evolution of the Bragg wavelength shift during the tests. Each step lasted between 30 and 40 s. To apply these loads, two masses of 100 g and 200 g were used, with uncertainties of 16 mg and 30 mg respectively. The Bragg wavelengths were measured using a BSI-108 data acquisition system, an 8-channel FBG interrogator developed

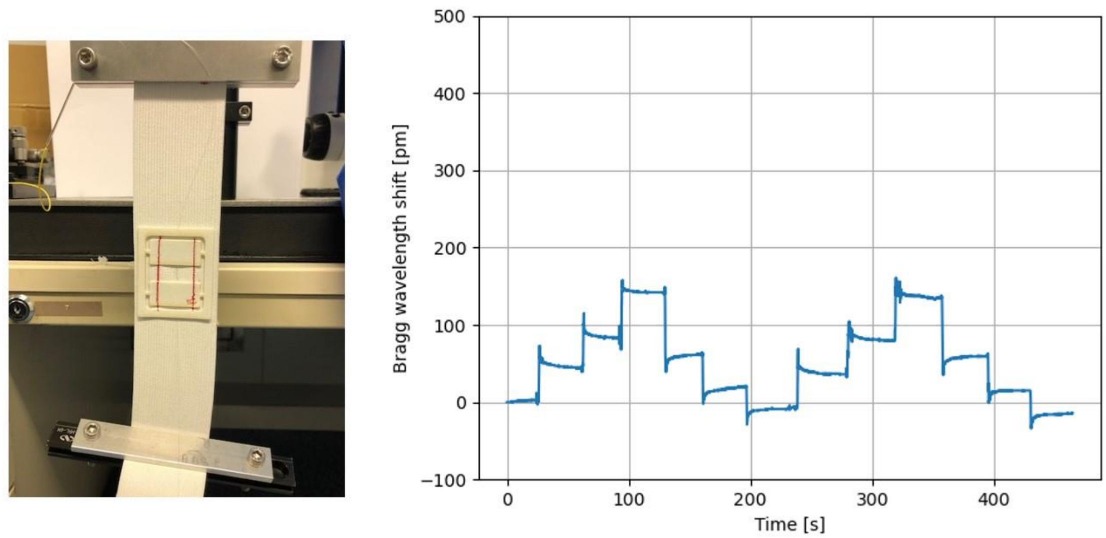

(a) (b)

Fig. 5. Pad configuration 1: (a) picture of the pad embedded into the elastic strip; (b) Bragg wavelength shift vs time for a tensile test of two cycles from 0 to 300 g by steps of 100 g.

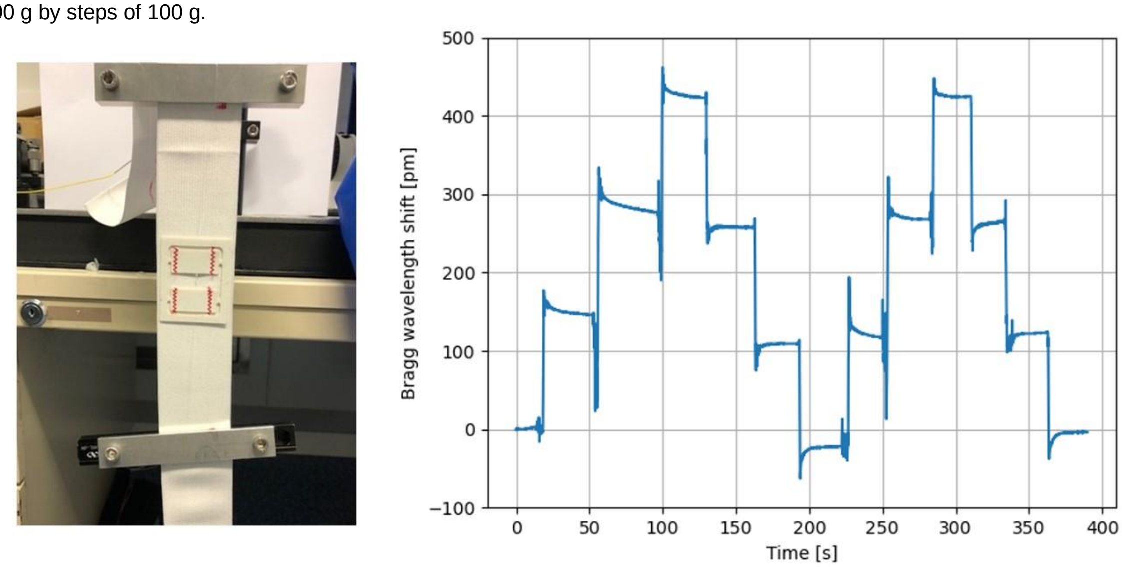

(a) (b)

Fig. 6. Pad configuration 2: (a) picture of the pad embedded into the elastic strip; (b) Bragg wavelength shift vs time for a tensile test of two cycles from 0 to 300 g by steps of 100 g.

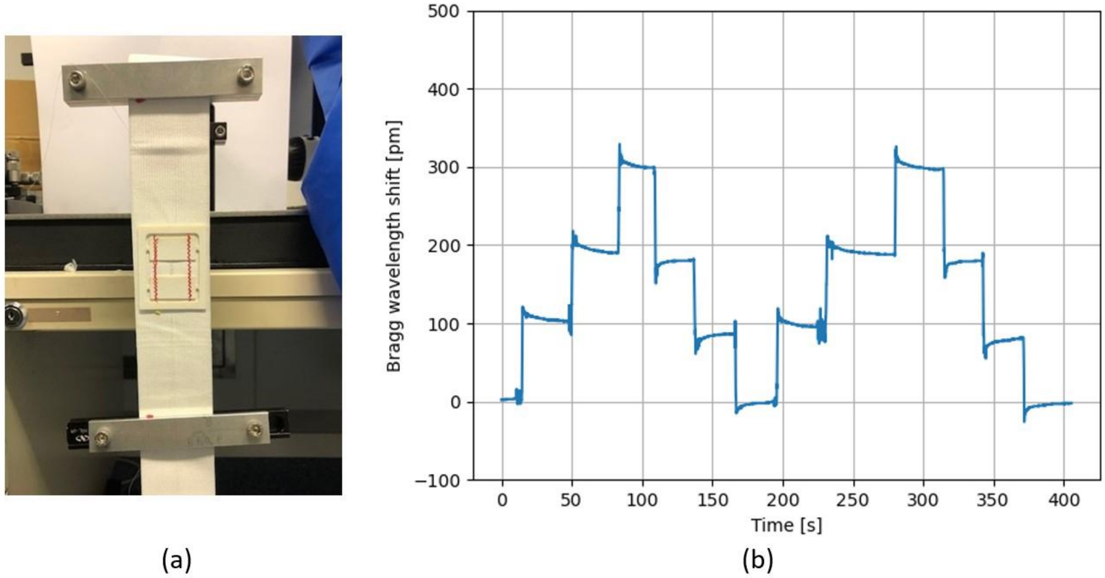

Fig. 7. Pad configuration 3: (a) picture of the pad embedded into the elastic strip; (b) Bragg wavelength shift vs time for a tensile test of two cycles from 0 to 300 g by steps of 100 g.

by B-SENS (Mons, Belgium). During the tests, the temperature remained constant (at room temperature, 20°C). Fig. 5(a) and 5(b) show a picture of the first pad configuration embedded into the elastic strip and the corresponding graph of the Bragg wavelength shift evolution, respectively. On the pictures, the seams are marked as the red thread.

With similar reasoning, the other two configurations are represented in Fig. 6 and 7. It comes out that the most sensitive configuration is the second one, so it will be chosen for the final design. This observation is coherent since it is the configuration for which the seams do not run along the piece of fabric between the mounts, which gives more freedom to the pad. The non-stability noticed between successive levels in the graphs comes from a manual change of the masses and is therefore not caused by a bad intrinsic mechanical behavior of the configuration.

IV. Calibration measurements

The calibration process involved determining the sensitivity of the sensing structure, which is the Bragg wavelength shift per unit of textile elongation. Due to the presence of the 3D-printed pad, the deformation of the fiber does not exactly match that of the elastic strip, resulting in a reduced sensitivity. To measure this sensitivity, a traction test was performed on the fabric strip at the *Civil Engineering and Structural Mechanics Department* of UMONS, and the Bragg wavelength shift was recorded for different levels of textile elongation. Fig. 8 is a picture of the elastic fabric strip undergoing the traction test. The measurements were also taken using a BSI-108 from B-SENS at a sampling frequency of 200 Hz. The test consisted in measuring the Bragg wavelength shift $\Delta\lambda$ for a textile elongation ΔL from 0 mm (rest state) to 90 mm by steps of 5 mm. The fabric strip was then released from 90 mm of elongation to the rest state by steps of 5 mm too. This traction test was performed at constant room temperature (20°C).

The graph showing the results can be found in Fig. 9. Due to the elastic nature of the strip, the elongation and release behaviors slightly differ from each other, inducing some hysteresis. Indeed, as the Bragg wavelength shift $\Delta\lambda$ is an image of the stress in the textile, this corresponds to the well-known stress-strain curves of elastic materials [17]. In elongation, the resulting sensitivity was calculated to be 12.2 pm/mm with an R^2 value of 0.98, as determined by the slope of the linear fit of the data. In release, the sensitivity is 11.7 pm/mm with an R^2 value of 0.98.

V. Validation testing

A. Sensitivity to compression

To demonstrate the sensor's capability of detecting compression in addition to elongation, a 7 s - stretching

Fig. 8. Picture of the elastic strip (outlined in red) during traction test.

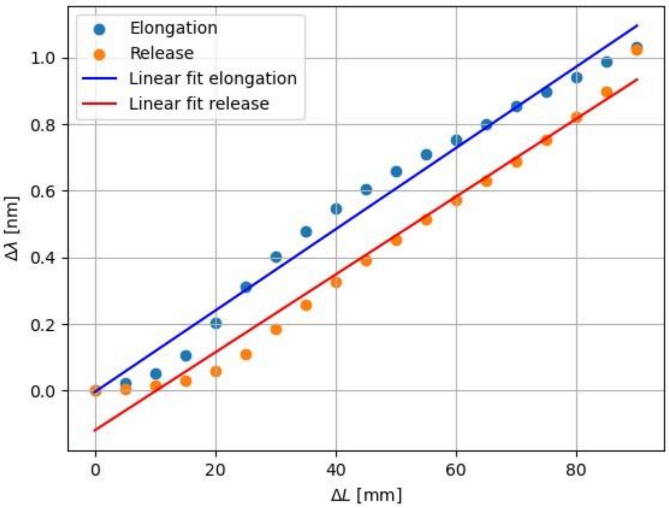

Fig. 9. Bragg wavelength shift vs textile elongation from tensile test.

followed by a 10 s - contraction was applied to an FBG of the fabric strip. The resulting Bragg wavelength versus time was recorded and presented in Fig. 10. It can be observed that the sensor was in a rest state between 0 s – 6 s and 26 s – 35 s.

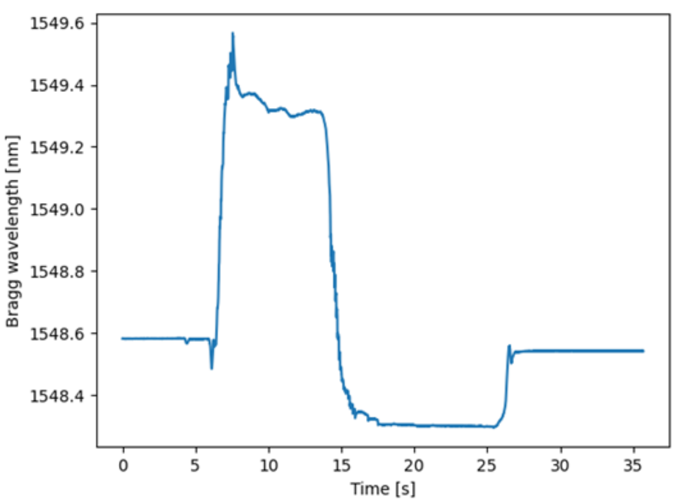

Fig. 10. Bragg wavelength temporal evolution during elongation-compression test.

B. Repeatability

Then, in order to demonstrate the effectiveness of the smart fabric strip in a dynamic setting, ten cycles of tension were applied, taking the fabric from its original state to an elongation of 90 mm. This was achieved in the same way as Fig. 8. Each cycle had a duration of approximately 130 s, with 80 s of elongation followed by 50 s of release. Cycles were carried out by imposing on the machine given lengths between both clamps that hold the fabric strip. Fig. 11 depicts the wavelength shift measured over time. The sensor's performance was consistent across all ten cycles, with the green lines indicating the highest and lowest levels observed. The mean value of all maxima was 1064.549 pm, with a standard deviation of 2.463 pm. The minimum mean value was -6.665 pm, with a standard deviation of 0.607 pm. These results demonstrate that the smart fabric strip has excellent and accurate repeatability.

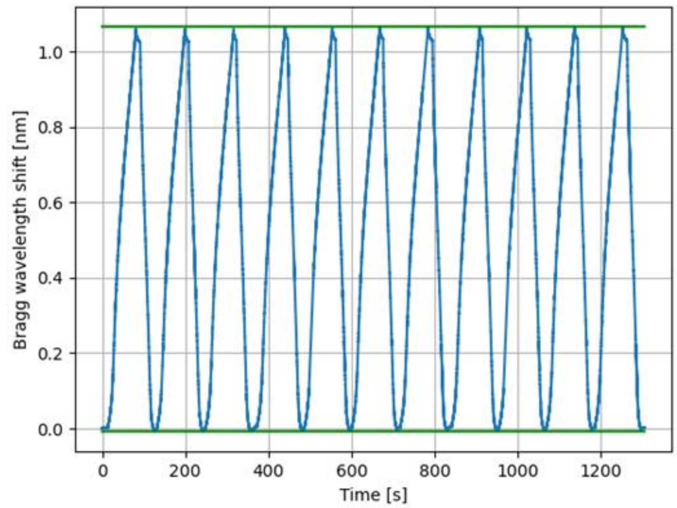

Fig. 11. Bragg wavelength shift vs time for ten traction-release cycles applied to the fabric strip.

C. Measurements for backbone monitoring

Finally, a validation was performed in a practical context of backbone monitoring. The smart textile was installed on a person, as shown by the picture in Fig. 12, with a scheme of the initial position, where red dots represent the FBG sensors, FBG 1 being the highest. The bottom end of the fabric is attached to the pants, to avoid a loose end that would imply no elongation. A qualitative analysis is performed according to different positions, followed by a quantitative test based on a calibration approach.

Measurements were taken by the *BSI-108* interrogator for four backbones positions. The obtained results, showing the Bragg wavelength shift of each sensor as a function of time, are displayed in Fig. 13 for the four positions, shown above each graph. The tests were done dynamically, i.e. from the initial position to the targeted position, then back to the initial position. The first three positions lasted a few seconds while the

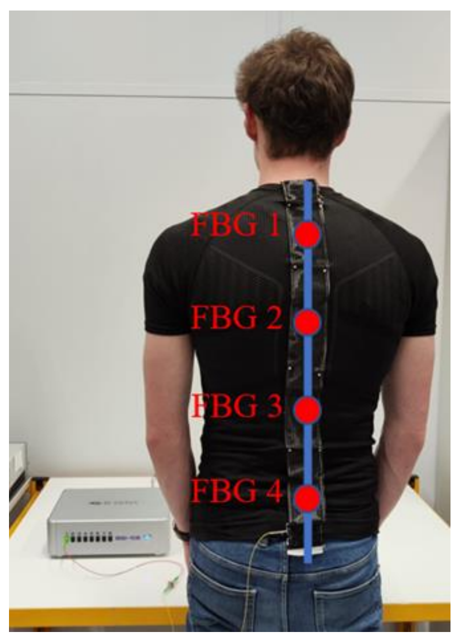

Fig. 12. Picture and scheme of the initial position of the backbone monitoring test.

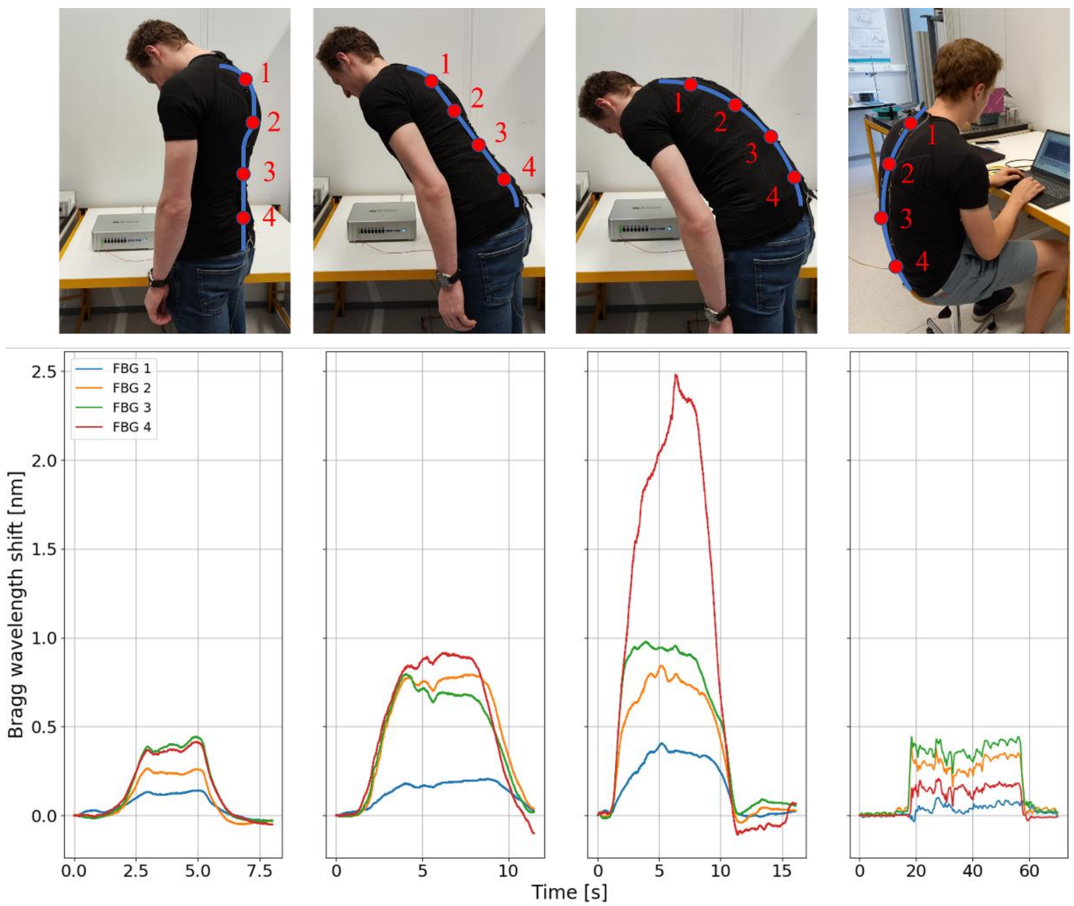

Fig. 13. Measured Bragg wavelength shift vs time in the frame of backbone monitoring according to four positions.

last one lasted about 40 seconds and was initially in a seated position with a straight back. For the analysis, the bending deformation has to be distinguished from the elongation deformation. Indeed, if the FBG sensor is bending but not elongating, it will be insensitive. For the first position, at the bottom of the bending (between FBG 2 and 3), the backbone shape induces an upwards traction to the rest of the strip (attached to the pants), which explains why FBG 3 and 4 show a higher elongation deformation. Then, for position 2, the first FBG is still in the bent part while the other three sensors undergo a similar elongation. In position 3, as the backbone is completely bent, the axial strain seen by the sensors increases from the top to the bottom and the Bragg wavelength shift of FBG 4 is the highest as it is located close to the strip attachment. Finally, position 4 enables strain relief at the FBG 4 location compared to the first three positions as the lower back rests on the chair. This explains why the FBG 4 curve is below these of FBG 2 and 3. Moreover, the oscillations that are present are caused by the volume variations of the thoracic cavity due to respiration.

A quantitative analysis can be performed based on these results. As every patient has a different morphology and as the fabric strip cannot be installed the exact same way for everybody, the FBGs will react differently. A calibration should thus be carried out after installation. For a given position that must be investigated on the patient, a threshold is defined above which the backbone position becomes problematic. For example, if the seated position must be examined, the focus is given on FBG 2 and 3 as they show the largest sensitivity, and the threshold of these sensors is set at 200 pm (this value is here chosen arbitrarily but must be discussed with the clinician). Above this value, the position is considered critical.

Our work so far has demonstrated the proof of concept of using distributed FBG sensors to dynamically monitor the backbone position. The performance evaluation, based on response time and tracking of the expected sensors position with respect to the backbone shape, shows satisfactory and promising results. This paves the way to the future real-time use of this technology provided that sufficient data are gathered so as to conceive the implementation of a machine-learning based demodulation process.

VI. Conclusion

In conclusion, this study presented a new design for a smart elastic fabric strip containing FBG sensors. The originality lies in the pad configuration allowing the FBG bonding in a pre-strained way. By means of tensile tests to investigate the sensor sensitivity, different configurations were considered and the most sensitive one was chosen for the final design, which consists in a fabric strip containing four FBG sensors, each affixed to a pad. The initial aim of the developed system was backbone monitoring, even if numerous other applications, e.g. requiring strain sensing on warping surfaces, can be targeted.

Then, calibration measurements were performed thanks to traction tests to determine the elastic fabric strip sensitivity. It comes out that the Bragg wavelength shifts by 12.2 pm per mm of fabric elongation and by 11.7 pm per mm in release. This result has been calculated using a 700 mm long strip. A compression of the textile validated the ability of the smart sensor to be sensitive to both compression and elongation. Ten traction-release cycles were then applied to the fabric strip to assess its performances in a dynamic environment. In the elongated states, the recorded Bragg wavelength shifts are very constant from one cycle to another, with a standard deviation of 2.463 pm. For every return to the original state (no elongation), the Bragg wavelength is also stable, characterized by a standard deviation of 0.607 pm. Finally, an actual backbone monitoring test demonstrated the good operation of the smart fabric strip in a practical context, by comparing results obtained for four backbone positions.

This developed smart elastic fabric strip offers numerous and various possibilities in terms of applications. Among them, it may include geotextiles or even strain sensing surrounding a deforming material, such as pipes for instance. For future works, the use of a small portable FBG interrogator could bring a handier touch to the sensing system. Also, machine-learning based algorithms are a track for improvement of the demodulation process.

References

[1] W. R. Habel and K. Krebber, “Fiber-optic sensor applications in civil and geotechnical engineering,” *Photonic Sensors*, vol. 1, no. 3. pp. 268–280, Sep. 2011. doi: 10.1007/s13320-011-0011-x.

[2] L. S. M. Alwis, K. Bremer, and B. Roth, “Fiber optic sensors embedded in textile-reinforced concrete for smart structural health monitoring: A review,” *Sensors*, vol. 21, no. 15. MDPI AG, Aug. 01, 2021. doi: 10.3390/s21154948.

[3] A. Biondi *et al.*, “Fiber Optic Sensing Textile for Strain Monitoring in Composite Substrates,” *Sensors*, vol. 22, no. 23, Dec. 2022, doi: 10.3390/s22239262.

[4] B. M. Quandt, L. J. Scherer, L. F. Boesel, M. Wolf, G. L. Bona, and R. M. Rossi, “Body-Monitoring and Health Supervision by Means of Optical Fiber-Based Sensing Systems in Medical Textiles,” *Adv Healthc Mater*, vol. 4, no. 3, pp. 330–355, Feb. 2015, doi: 10.1002/adhm.201400463.

[5] A. Grillet *et al.*, “Optical fiber sensors embedded into medical textiles for healthcare monitoring,” in *IEEE Sensors Journal*, Jul. 2008, pp. 1215–1222. doi: 10.1109/JSEN.2008.926518.

[6] D. Lo Presti *et al.*, “Smart Textile Based on 12 Fiber Bragg Gratings Array for Vital Signs Monitoring,” *IEEE Sens J*, vol. 17, no. 18, pp. 6037–6043, Sep. 2017, doi: 10.1109/JSEN.2017.2731788.

[7] Z. Gong *et al.*, “Wearable fiber optic technology based on smart textile: A review,” *Materials*, vol. 12, no. 20. MDPI AG, Oct. 01, 2019. doi: 10.3390/ma12203311.

[8] Y. Koyama, M. Nishiyama, and K. Watanabe, “Smart textile using hetero-core optical fiber for heartbeat and respiration monitoring,” *IEEE Sens J*, vol. 18, no. 15, pp. 6175–6180, Aug. 2018, doi: 10.1109/JSEN.2018.2847333.

[9] H. Wang *et al.*, “SleepSense: Smart Pillow With Pressure-Sensitive FBG-Embedded Silicone Buttons,” *IEEE Sens J*, vol. 23, no. 17, pp. 19324–19331, 2023, doi: 10.1109/JSEN.2023.3295114.

[10] B. Kaur, S. Kumar, and B. K. Kaushik, “Novel Wearable Optical Sensors for Vital Health Monitoring Systems—A Review,” *Biosensors*, vol. 13, no. 2. MDPI, Feb. 01, 2023. doi: 10.3390/bios13020181.

[11] J. Witt *et al.*, “Medical textiles with embedded fiber optic sensors for monitoring of respiratory movement,” *IEEE Sens J*, vol. 12, no. 1, pp. 246–254, 2012, doi: 10.1109/JSEN.2011.2158416.

[12] M. Ciocchetti *et al.*, “Smart textile based on fiber bragg grating sensors for respiratory monitoring: Design and preliminary trials,” *Biosensors (Basel)*, vol. 5, no. 3, pp. 602–615, 2015, doi: 10.3390/bios5030602.

[13] C. Massaroni *et al.*, “Design and Feasibility Assessment of a Magnetic Resonance-Compatible Smart Textile Based on Fiber Bragg Grating Sensors for Respiratory Monitoring,” *IEEE Sens J*, vol. 16, no. 22, pp. 8103–8110, Nov. 2016, doi: 10.1109/JSEN.2016.2606487.

[14] D. Lo Presti *et al.*, “Cardio-respiratory monitoring in archery using a smart textile based on flexible fiber bragg grating sensors,” *Sensors (Switzerland)*, vol. 19, no. 16, Aug. 2019, doi: 10.3390/s19163581.

[15] L. Shen *et al.*, “WaveFlex Sensor: Advancing Wearable Cardiorespiratory Monitoring with Flexible Wave-Shaped Polymer Optical Fiber,” *IEEE Journal of Selected Topics in Quantum Electronics*, pp. 1–8, 2023, doi: 10.1109/JSTQE.2023.3319581.

[16] M. Zaltieri *et al.*, “Assessment of a Multi-Sensor FBG-Based Wearable System in Sitting Postures Recognition and Respiratory Rate Evaluation of Office Workers,” *IEEE Trans Biomed Eng*, vol. 70, no. 5, pp. 1673–1682, May 2023, doi: 10.1109/TBME.2022.3225065.

[17] L. Mullins, “Softening of Rubber by Deformation,” *Rubber Chemistry and Technology*, vol. 42, no. 1, 1969, doi: 10.5254/1.3539210.